

# Numerical modelling of bore propagation and run-up on sloping beaches using a MacCormack TVD scheme

## Modélisation numérique de la propagation d'un ressaut et d'un front sur une plage inclinée avec un schéma MacCormack TVD

S. VINCENT and J-P. CALTAGIRONE, *Modélisation Avancée des Systèmes Thermiques et écoulements Réels, Université Bordeaux 1, Avenue Pey-Berland, BP 108 - 33402 Talence, France*

P. BONNETON, *Department of Geology and Oceanography, URA CNRS 197, University of Bordeaux 1, 33405 Talence, France*

### ABSTRACT

A MacCormack TVD scheme is presented for the computation of Saint-Venant equations, in the context of coastal hydrodynamics. The dam-break problem on wet and dry bottoms is used to evaluate and discuss the performances of the scheme. A run-up simulation on a sloping beach is then presented and a comparison using an analytical solution is made. Finally, a bore propagation on a sloping beach is computed.

### RÉSUMÉ

Un schéma MacCormack TVD est présenté pour la résolution numérique des équations de Saint-Venant dans le cadre de l'hydrodynamique côtière. Le problème du lâché de barrage sur fonds secs et mouillés est abordé pour évaluer et discuter les performances du schéma. Une simulation de propagation d'un front d'eau sur une plage inclinée est alors présentée et une comparaison avec une solution analytique est effectuée. Finalement, la propagation d'un ressaut sur une plage est simulée.

### 1 Introduction

The Saint-Venant (SV) shallow water equations are relevant to describe waves in the coastal zone where the water depth is shallow in comparison to the characteristic horizontal lengthscale of the motion. On a large scale, they can be applied to the analysis of tidal oscillations or to the study of wave damage due to tsunamis or storm waves. The SV equations are also appropriate to describe phenomena on a smaller scale, such as broken-wave (bore) propagation and run-up on beaches, which play a major role in sediment transport and beach evolution. In both cases, a correct estimation of levels and velocity fields in the very shallow and transitional dry regions is a difficult numerical problem, essentially because strong velocity gradients occur near the run-up point, as demonstrated by Carrier and Greenspan [4] and Hibberd and Peregrine [10]. Other difficulties arise from the non-linearity and hyperbolicity of the SV equations which give rise to the appearance of discontinuous solutions, which are the mathematical counterpart of physical phenomena such as bores.

To compute waves near the shoreline and bore propagation it is necessary to use a shock-capturing numerical method. Hibberd and Peregrine [10] and Kobayashi et al. [12] have chosen the Lax-Wendroff scheme, which has become very popular for solving hyperbolic systems. This explicit finite-difference scheme, second-order accurate in space and time, has been successfully applied to solve numerous problems in gas dynamics. However, in the presence of fronts, the dispersive properties of this scheme introduce spurious numerical oscillations. To reduce these high-frequency oscillations which tend to appear at the rear of the wave front, Hibberd and Peregrine [10] and Kobayashi et al. [12]

included an additional dissipative term. As noticed by Hirsh [11], this correction requires empiricism.

An alternative to this method is to use a TVD (total variation diminishing, Harten [9]) scheme, which represents a rational method for the determination of artificial dissipation terms. In this paper, we report the implementation of this method onto the MacCormack time splitting scheme, and the ability of the resulting TVD scheme to simulate bore propagation, strong velocity gradients near the run-up point, as well as dry/wet zone flow transition.

### 2 TVD MacCormack scheme

Referring to the definition sketch (figure 1), the one-dimensional SV equations can be expressed in a vectorial form as follows:

$$\frac{\partial \mathbf{q}}{\partial t} + \frac{\partial \mathbf{F}}{\partial x} = \mathbf{S} \quad (1)$$

where

$$\mathbf{q} = \begin{pmatrix} h \\ hu \end{pmatrix}, \quad \mathbf{F} = \begin{pmatrix} hu \\ hu^2 + \frac{g}{2} h^2 \end{pmatrix}, \quad \mathbf{S} = \begin{pmatrix} 0 \\ -gh \frac{\partial Z_f}{\partial x} \end{pmatrix}$$

$h(x,t)$  is the total depth of water,  $u(x,t)$  is the averaged velocity on the water depth,  $Z_f$  is the bed elevation and  $g$  is the gravitational acceleration.

To precisely calculate the wave propagation, we have implemented a classical hyperbolic solving method, the MacCormack scheme, which was used successfully by Garcia and Kahawita [6]

Revision received April 21, 2000. Open for discussion till August 31, 2001.

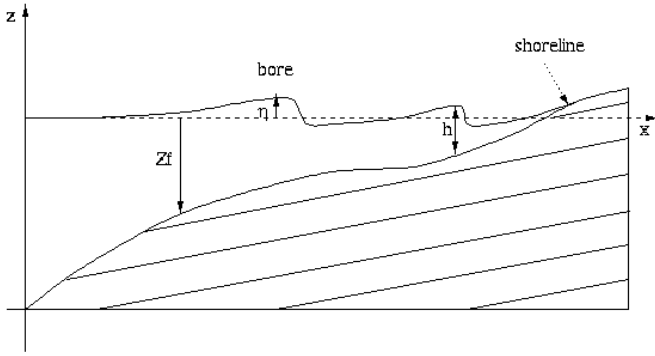


Fig. 1. Definition sketch

for solving SV equations. As explained by LeVeque and Yee [13] and Garcia-Navarro et al. [7], the main reason for choosing the predictor-corrector step instead of the one-step Lax-Wendroff formulation is that the former provides a natural way to include the source terms  $\mathbf{S}$  keeping second order accuracy in time and space, whereas the one-step Lax-Wendroff scheme needs a specific treatment to do so (semi-implicit resolution method for example). The McCormack scheme obtained yields very good solutions in regular zones, but brings about oscillations when strong water height or velocity gradients occur. Following the work of Yee ([21]) for the Navier-Stokes compressible equations, we have modified the McCormack scheme with a TVD flux correction to make it non-oscillating. The TVD McCormack scheme so obtained retains second-order precision in space and time in regular zones and is oscillation-free across discontinuities. In this paper we present the one-dimensional algorithm. The two-dimensional one can be obtained in a straightforward manner and has been described by Yee ([21]) for Navier-Stokes equations, and Bonneton et al. [2] for SV equations.

Let  $\mathbf{q}^n$  be the numerical solution of equation (1) at  $x=i\Delta x$  and  $t=n\Delta t$ , with  $\Delta x$  the spatial mesh size and  $\Delta t$  the time step;  $\lambda=\Delta t/\Delta x$ .  $q^l$ ,  $F^l$ ,  $S^l$  correspond to the  $l^{\text{th}}$  component ( $l=1,2$ ) of the previously defined vectors. The TVD McCormack scheme can be expressed in three steps:

(a) predictor step

$$\mathbf{q}_i^1 = \mathbf{q}_i^n - \lambda (\mathbf{F}_{i+1}^n - \mathbf{F}_i^n) + \Delta t \mathbf{S}_i^n$$

(b) corrector step

$$\mathbf{q}_i^2 = \frac{1}{2} [\mathbf{q}_i^1 + \mathbf{q}_i^n - \lambda (\mathbf{F}_i^1 - \mathbf{F}_{i-1}^1) + \Delta t \mathbf{S}_i^1]$$

(c) TVD step

$$\mathbf{q}_i^{n+1} = \mathbf{q}_i^2 - \lambda \left( \mathbf{H}_{i+\frac{1}{2}}^{n,T} - \mathbf{H}_{i-\frac{1}{2}}^{n,T} \right) \quad (2)$$

where the McCormack TVD fluxes  $\mathbf{H}^T$  are build on the combinaison of Upwind of first order and Lax-Wendroff approximations as follows

$$\mathbf{H}_{i+\frac{1}{2}}^T = \left( 1 - \Psi_{i+\frac{1}{2}} \right) \left( \mathbf{H}_{i+\frac{1}{2}}^H - \mathbf{H}_{i-\frac{1}{2}}^L \right)$$

The notation  $i+\frac{1}{2}$  corresponds to quantities estimated at the mesh interface  $(i,i+1)$ .  $\Psi_{i+\frac{1}{2}}$  is a diagonal matrix whose elements correspond to limiter varying from 0 and 1. Each component of  $\Psi_{i+\frac{1}{2}}$  lead to an hybrid solution between low ( $\Psi^{l,l}=0$ ) and high ( $\Psi^{l,l}=1$ ) order. The subscripts L, H and T refers to low order, high order and TVD fluxes.

The steps (a) and (b) describe the classical MacCormack scheme whereas the step (c) is a TVD flux correction. If we interpret  $\mathbf{q}_i^2$  as a solution resulting from a conservative discretisation of high order, we have

$$\mathbf{q}_i^2 = \mathbf{q}_i^n - \lambda \left( \mathbf{H}_{i+\frac{1}{2}}^H - \mathbf{H}_{i-\frac{1}{2}}^H \right) \quad (3)$$

Using equations (2-3), the MacCormack TVD scheme can be re-written as

$$\mathbf{q}_i^{n+1} = \mathbf{q}_i^n - \lambda \left( \mathbf{H}_{i+\frac{1}{2}}^H - \mathbf{H}_{i-\frac{1}{2}}^H \right) - \lambda \left( \mathbf{H}_{i+\frac{1}{2}}^T - \mathbf{H}_{i-\frac{1}{2}}^T \right) \quad (4)$$

If we extract a numerical flux from equation (4),

$$\mathbf{H}_{i+\frac{1}{2}}^{TVD} = \mathbf{H}_{i+\frac{1}{2}}^H + \left( 1 - \Psi_{i+\frac{1}{2}} \right) \left( \mathbf{H}_{i+\frac{1}{2}}^H - \mathbf{H}_{i-\frac{1}{2}}^L \right)$$

we recover the general formulation of conservative TVD schemes

$$\mathbf{q}_i^{n+1} = \mathbf{q}_i^n - \lambda \left( \mathbf{H}_{i+\frac{1}{2}}^{TVD} - \mathbf{H}_{i-\frac{1}{2}}^{TVD} \right)$$

According for example to the work of Leveque [13], the numerical fluxes coming from first order and Lax-Wendroff discretisations can be expressed as

$$\mathbf{H}_{i+\frac{1}{2}}^L = \frac{1}{2} \left[ \mathbf{A}_{i+\frac{1}{2}} \left( \mathbf{q}_{i+1}^n + \mathbf{q}_i^n \right) - \left| \mathbf{A}_{i+\frac{1}{2}} \right| \left( \mathbf{q}_{i+1}^n - \mathbf{q}_i^n \right) \right] \quad (5)$$

$$\mathbf{H}_{i+\frac{1}{2}}^H = \frac{1}{2} \left[ \mathbf{A}_{i+\frac{1}{2}} \left( \mathbf{q}_{i+1}^n + \mathbf{q}_i^n \right) - \lambda \left| \mathbf{A}_{i+\frac{1}{2}} \right|^2 \left( \mathbf{q}_{i+1}^n - \mathbf{q}_i^n \right) \right] \quad (6)$$

where  $\mathbf{A} = \frac{\partial \mathbf{F}}{\partial \mathbf{q}}$  is the flux Jacobian matrix,  $\left| \mathbf{A}_{i+\frac{1}{2}} \right| = \mathbf{R}_{i+\frac{1}{2}} \Gamma_{i+\frac{1}{2}} \mathbf{R}_{i+\frac{1}{2}}^{-1}$ ,  $\mathbf{R}_{i+\frac{1}{2}}$  is the right-eigenvector matrix associated to  $\mathbf{A}$  and  $\Gamma_{i+\frac{1}{2}}$  the corresponding diagonal eigenvalues matrix.

Combining (5) and (6), we get

$$\mathbf{H}_{i+\frac{1}{2}}^H - \mathbf{H}_{i+\frac{1}{2}}^L = \frac{1}{2} \left[ \left| \mathbf{A}_{i+\frac{1}{2}} \right| - \lambda \left| \mathbf{A}_{i+\frac{1}{2}} \right|^2 \right] (\mathbf{q}_{i+1}^n - \mathbf{q}_i^n)$$

Developing with respect to the basis of the characteristic speeds, we obtain

$$\mathbf{H}_{i+\frac{1}{2}}^H - \mathbf{H}_{i+\frac{1}{2}}^L = \frac{1}{2} \mathbf{R}_{i+\frac{1}{2}} \left[ \left| \Gamma_{i+\frac{1}{2}} \right| - \lambda \left| \Gamma_{i+\frac{1}{2}} \right|^2 \right] \mathbf{R}_{i+\frac{1}{2}}^{-1} (\mathbf{q}_{i+1}^n - \mathbf{q}_i^n)$$

and finally

$$\mathbf{q}_i^{n+1} = \mathbf{q}_i^n - \lambda \left( \mathbf{R}_{i+\frac{1}{2}}^n \Phi_{i+\frac{1}{2}}^n - \mathbf{R}_{i-\frac{1}{2}}^n \Phi_{i-\frac{1}{2}}^n \right)$$

where  $\Phi_{i+\frac{1}{2}} = \mathbf{R}_{i+\frac{1}{2}}^{-1} \mathbf{H}_{i+\frac{1}{2}}^r$ .

We can express each component  $l$  of  $\Phi_{i+\frac{1}{2}}^{n+1}$  as

$$\left( \phi_{i+\frac{1}{2}}^l \right) = \frac{1}{2} \left[ \left| a_{i+\frac{1}{2}}^l \right| - \lambda \left( a_{i+\frac{1}{2}}^l \right)^2 \right] \left( \alpha_{i+\frac{1}{2}}^l - Q_{i+\frac{1}{2}}^l \right)$$

where  $a_{i+\frac{1}{2}}^l$  represents the  $l$ th component of the vector of local

characteristic speeds,  $\alpha_{i+\frac{1}{2}} = \mathbf{R}_{i+\frac{1}{2}}^{-1} (\mathbf{q}_{i+1} - \mathbf{q}_i)$ , and

$Q_{i+\frac{1}{2}} = \text{minmod} \left( \alpha_{i-\frac{1}{2}}^l, \alpha_{i+\frac{1}{2}}^l, \alpha_{i+\frac{3}{2}}^l \right)$  is the flux limiter corresponding to

$\Psi^{l,l}$ . Other limiters such as

$$Q_{i+\frac{1}{2}}^l = \text{minmod} \left( \alpha_{i-\frac{1}{2}}^l, \alpha_{i+\frac{1}{2}}^l \right) + \text{minmod} \left( \alpha_{i+\frac{1}{2}}^l, \alpha_{i+\frac{3}{2}}^l \right) - \alpha_{i+\frac{1}{2}}^l$$

or

$$Q_{i+\frac{1}{2}}^l = \text{minmod} \left( 2\alpha_{i-\frac{1}{2}}^l, 2\alpha_{i+\frac{1}{2}}^l, 2\alpha_{i+\frac{3}{2}}^l, \frac{1}{2} \left[ \alpha_{i-\frac{1}{2}}^l + \alpha_{i+\frac{3}{2}}^l \right] \right)$$

can be found in literature (Hirsch [11], Yee [21]), but they appear to be more diffusive. The minmod function is defined by

$$\text{minmod}(a_1, a_2, \dots, a_n) = \begin{cases} 0 & \text{if } \exists(i, j) / \text{sign}(a_i) \neq \text{sign}(a_j) \\ \text{sign}(a_1) \min(|a_i|) & \text{else} \end{cases}$$

At the interface of the meshes  $\mathbf{q}_{i+\frac{1}{2}}$  is determined by Roe's [17]

averaging, which is an approximate Riemann solver (cf. Appendix):

$$h_{i+\frac{1}{2}} = \frac{h_{i+1} + h_i}{2}$$

$$u_{i+\frac{1}{2}} = \frac{\sqrt{h_{i+1}} u_{i+1} + \sqrt{h_i} u_i}{\sqrt{h_{i+1}} + \sqrt{h_i}}$$

The solver a)-b)-c) is easy to implement and yields good results. Similar approach have been implemented with success by Garcia et al. [7] to solve the SV equations on flood processes and classical hydraulic problems. To avoid the scheme converging to non-

physical solutions, a classical entropy correction function  $\eta$  has been used:

$$\eta(z) = \begin{cases} |z| & \text{if } |z| \geq \varepsilon \\ \frac{z^2 + \varepsilon^2}{2\varepsilon} & \text{if } |z| < \varepsilon \end{cases} \quad (7)$$

Thanks to (7), each component of  $\Phi_{i+\frac{1}{2}}$  can be rewritten as

$$\left( \phi_{i+\frac{1}{2}}^l \right) = \frac{1}{2} \left[ \eta \left( a_{i+\frac{1}{2}}^l \right) - \lambda \left( a_{i+\frac{1}{2}}^l \right)^2 \right] \left( \alpha_{i+\frac{1}{2}}^l - Q_{i+\frac{1}{2}}^l \right)$$

In our problem, the MacCormack TVD scheme brings the same entropic solution with the entropy correction associated to a very small  $\varepsilon$  and without this correction.

### 3 Dry zones and varying topography

The presence of dry zones is a crucial numerical problem to be solved. Different techniques are commonly used in literature: either you calculate only where the water is present and you have to manage the dry/wet interface (Zhao and al. [23]) or you calculate everywhere, imposing a thin water layer  $h_d$  in the dry zones (Wang [19]). We chose to use the second method: in the dry zones, we take  $u = 0 \text{ m.s}^{-1}$  and  $h_d = 10^{-4} \text{ m}$  whereas at the shoreline (wet meshes next to dry meshes) a specific treatment is applied in the momentum equation to the discretization of the horizontal gradient of the surface elevation so that

$$gh \frac{\partial \eta}{\partial x} = gh \left( \frac{\partial h}{\partial x} + \frac{\partial Z_f}{\partial x} \right)$$

It consists in omitting the landward spatial differences of this term in the predictor and corrector steps.

The study of flows dealing with non-horizontal bottom involves the presence of a source term in the SV equations. When the bottom topography shows strong variations, it is necessary to develop a special treatment of the source term to avoid the generation of artificial numerical waves due to bottom variations. Several numerical methods exists such as extracting the term

$$\frac{g}{2} h^2$$

from the flux function  $\mathbf{q}$  and discretize it to verify compatibility with  $\mathbf{S}$  (Nujic [16]), or building Well-Balanced laws based on exact Riemann solvers (Chinnayya and Le Roux [5]). Our purpose is to build a numerical model to compute broken wave in the inner surf zone over sandy beaches which are usually characterised by even profiles. Balancing the space derivatives

$$\frac{1}{2} \frac{\partial gh^2}{\partial x} \text{ and } -gh \frac{\partial Z_f}{\partial x}$$

by a Finite Volume discretisation as follows

$$\begin{cases} \frac{1}{2} \frac{\partial gh^2}{\partial x} = \frac{1}{2} g \frac{h_{i+1}^2 - h_i^2}{\Delta x} = \frac{1}{2} g (h_{i+1} + h_i) \frac{(h_{i+1} - h_i)}{\Delta x} \\ -gh \frac{\partial Z_f}{\partial x} = -g (h_{i+1} - h_i) \frac{(Z_{f,i+1} - Z_{f,i})}{\Delta x} \end{cases}$$

our numerical model provide accurate solutions on linear slopes (see section 5) and on real sandy beach profiles varying smoothly (Bonneton et al [3]).

#### 4 Tests on dam-break problem

To validate the shock-capturing ability of our method, we present two frictionless transcritical flow problems: the dam-break on wet bottom and the dam-break on dry bottom. The dam-break simulation is a good way of validating our model because we are familiar with analytical solutions from several articles discussing this test (Nujic [16], Glaister [8], Zhao et al. [23] for example).

##### 4.1 Dam-break on wet bottom

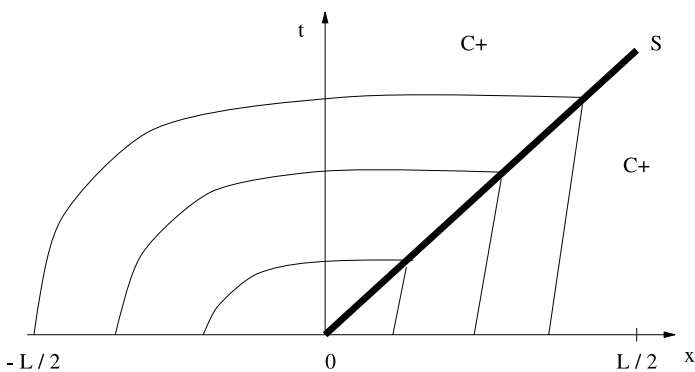
At the beginning of the calculations, the dam-break on wet bottom is represented by a water step free surface. The upstream part  $h_1$  corresponds to a water reserve behind a dam, whereas the downstream part  $h_2$  represents a steady water layer.

Figure 2 presents a characteristic analysis of this problem. The solution is split into a subcritical flow from  $x = -L/2$  to  $x = 0$  ( $Fr < 1$ , where  $Fr = \frac{u}{\sqrt{gh}}$  is the Froude number), where  $L$  is the domain length, and a supercritical flow from  $x = 0$  to  $x = L/2$  ( $Fr > 1$ ), where a shock spreads from  $x = 0$  to  $x = L/2$  (see fig. 2-left) and an expansion wave appears in the subcritical flow between A and B (fig. 2-right). A sonic point is located in  $x = 0$ .

Leading the characteristic theory, the analytical solution is then:

- from  $x = -L/2$  to OA (OA is the  $x = -\sqrt{gh_1} t$  curve), the analytical solution is  $u = 0$  and  $h = h_1$ .
- from OA to OB (OB is the  $x = -\sqrt{gh_2} t$  curve), we get

$$u_s = \left( \frac{2}{3} \sqrt{gh_1} + \frac{2x}{3t} \right) \text{ and } h = \frac{\left( \frac{2}{3} \sqrt{gh_1} - \frac{x}{3t} \right)^2}{g}$$



- from OB to OS (OS corresponds to the  $x = s t$  curve, where  $s$  is the shock velocity), the solutions  $h_s$  and  $u_s$  left to the shock are obtained solving the following system

$$\begin{cases} u_s + 2\sqrt{gh_s} - 2\sqrt{gh_1} = 0 \text{ (Riemann invariant)} \\ s(h_2 - h_s) - (h_2 u_2 - h_s u_s) = 0 \text{ (flux continuity through the shock)} \\ s(h_2 u_2 - h_s u_s) - \left( \frac{(h_2 u_2)^2}{h_2} + \frac{gh_2^2}{2} \right) + \left( \frac{(h_s u_s)^2}{h_s} + \frac{gh_s^2}{2} \right) = 0 \text{ (flux continuity through the shock)} \end{cases}$$

- from OS to  $x = L/2$ , the solution is  $u = 0$  and  $h = h_2$

Initially, the dam is located at  $x = 50$  m with  $L = 100$  m. The water depth upstream is  $h_1 = 10$  m whereas the water depth downstream is  $h_2 = 1$  m. A grid of 200 points was used with  $\Delta t = 0.01$  s. A comparison between the analytical solution and the numerical simulations with the Mac-Cormack TVD scheme are shown on fig. 3 and 4. The approximate solution is close to the analytical one, especially in the regular zones, where the TVD scheme is of high order. In the expansion and shock zones, even if small discrepancies exist between the results because of the order one of the scheme, one can see that the numerical solution fits well the characteristic theory. We can observe that the sonic point located in  $x = 50$  m is well calculated (fig. 3 and 4). Near velocity or depth discontinuities, no oscillation appears: the TVD property is verified. The results proposed by Nujic [16] using Lax-Friedrichs TVD and ENO schemes and by Zhao [23] with an Osher scheme are comparable to our solutions.

##### 4.2 Dam-break on dry bottom

This test is very interesting because it corresponds to wave propagation on dry bottom. The upstream part  $h_1$  corresponds to a water reserve behind a dam, whereas the downstream part  $h_2$  is a dry zone. The analytical solution is deduced from the characteristic theory (fig. 5), as in the previous dam test (Whitham [20]).

The analytical solution is separated into three zones:

- from  $x = -L/2$  to OA, we obtain a steady state corresponding to initial conditions. OA is the  $x = -\sqrt{gh_1} t$  curve. The analytical solution is  $u = 0$  and  $h = h_1$

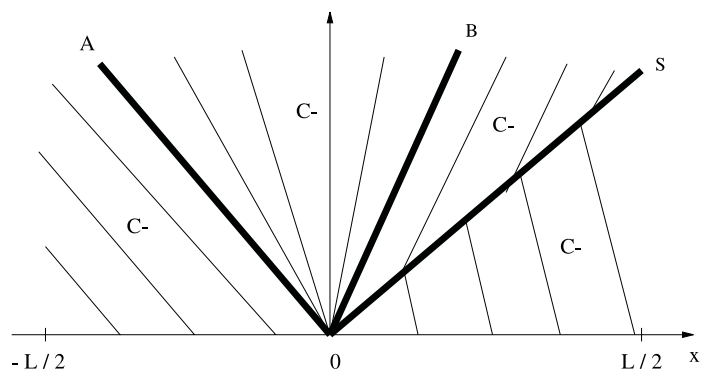


Fig. 2. Left: description of the  $C_+$  characteristics curves, associated with the characteristic speed  $u + \sqrt{gh}$  in the  $(x,t)$  plan. Initially, the dam-break is located in  $x=0$ . A shock wave S appears. Right: description of the  $C_-$  characteristics curves, associated with the characteristic speed  $u - \sqrt{gh}$  in the  $(x,t)$  plan. An expansion wave appears between A and B.

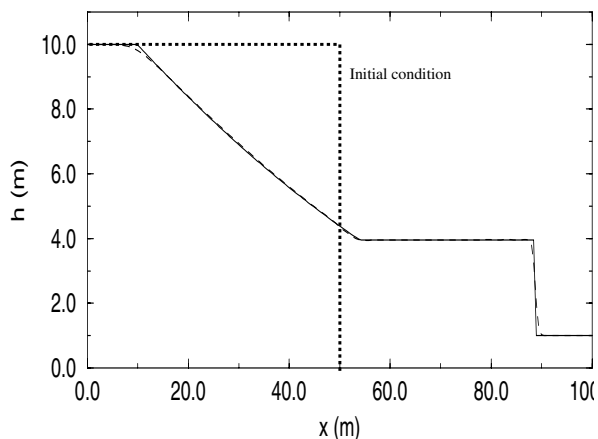


Fig. 3. Water surface profile at  $t = 4$  s - Comparison between the analytical solution (—) and the simulation (- - -) with the MacCormack TVD scheme. 200 grid points are computed with  $\Delta t = 0.01$ .

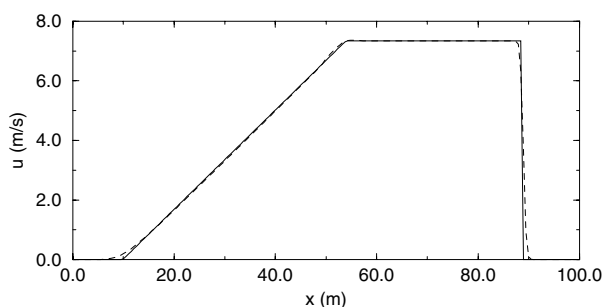


Fig. 4. Velocity profile at  $t = 4$  s - Comparison between the analytical solution (—) and the simulation (- - -) with the MacCormack TVD scheme. 200 grid points are computed with  $\Delta t = 0.01$ .

- from OA to OS, we get an expansion wave containing the sonic point  $x = 0$ . OS is the  $x = 2\sqrt{gh_1}t$  curve. The solution is

$$u = \left( \frac{2}{3}\sqrt{gh_1} + \frac{2x}{3t} \right)$$

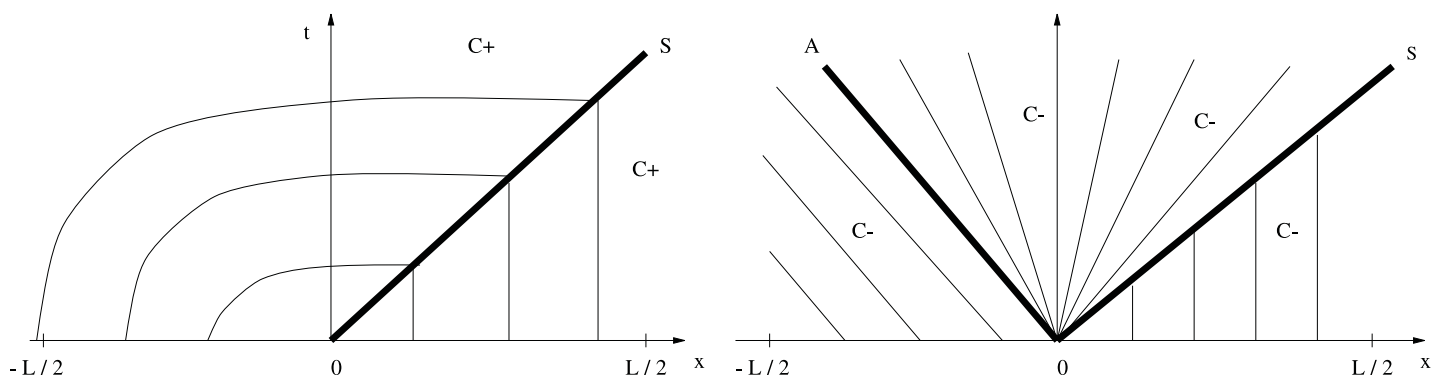


Fig. 5. Left: description of the  $C_+$  characteristics curves, associated with the characteristic speed  $u + \sqrt{gh}$  in the  $(x,t)$  plan - Initially, the dam-break is located in  $x=0$  - an expansion wave appears between A and  $x = 0$ . Right: description of the  $C_-$  characteristics curves, associated with the characteristic speed  $u - \sqrt{gh}$  in the  $(x,t)$  plan - a shock wave appears in S.

and

$$h = \frac{\left( \frac{2}{3}\sqrt{gh_1} - \frac{x}{3t} \right)^2}{g}$$

- from OS to  $x = L/2$ , we obtain a steady state corresponding to initial conditions. The solution is  $u = 0$  and  $h = h_2$ .

The initial condition corresponds to a dam located at  $x = 5$  m with  $L = 100$  m. The water depth upstream is  $h_1 = 10$  m whereas the water depth downstream is  $h_2 = 0$  m. We use a grid of 200 points with  $\Delta t = 0.01$  s. If we compare the analytical solution and the numerical simulations with the MacCormack TVD scheme (fig. 6 and 7), we can observe that the approximate solution is very similar to the analytical one. The transition point between the wet zone and the dry zone is correctly calculated with respect to  $h$ , but some difficulties appear on the velocity. Indeed, as the solution is similar to a peak in this zone, the TVD scheme becomes an order 1 one and is diffusive. More than that, the thin water layer kept in the dry zone modifies the dynamics near the transition point creating approximation errors, which cause a delay in the numerical solution. As explained by Ambrosi [1], when the elevation goes to 0, the velocity retains a finite value and the Froude becomes infinity. We then understand that the SV equation system loses its strict hyperbolicity and the two eigenvalues collapse into  $\lambda = u$ . In fact, the characteristic theory cannot be applied in the wet/dry transition point. When we do so, we introduce a small error on one point of the solution. Nevertheless, the results are globally accurate and totally non-oscillating. The results obtained are comparable to Ambrosi's ones.

## 5 Run-up and back-wash of a non-breaking wave

A non-linear and non-breaking standing wave reflecting on a constant sloping beach can correspond to a long period wave (infragravity waves for example), alternatively running up and back washing on a dry beach zone. The transition between the dry and wet zones makes the numerical problem rather difficult to approximate. In the frictionless problem, analytical solutions exist (Carrier and Greenspan [4], Mei [15]).

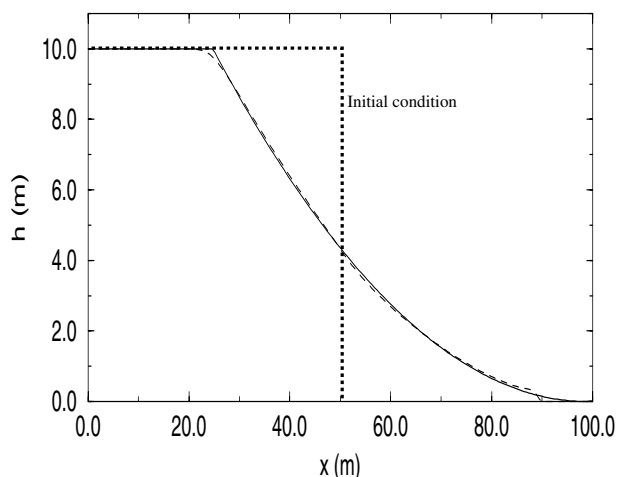


Fig. 6. Water surface profile at  $t = 2.5$  s - Comparison between the analytical solution (—) and the simulation (- - -) with the MacCormack TVD scheme. 200 grid points are computed with  $\Delta t = 0.01$ .

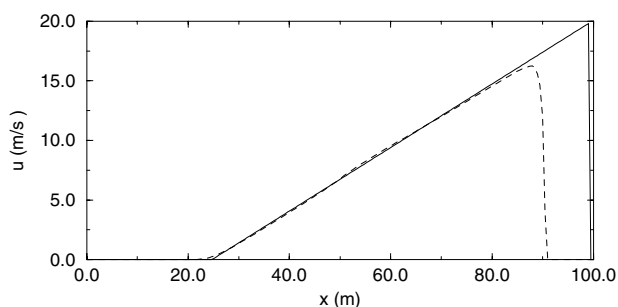


Fig. 7. Velocity profile at  $t = 2.5$  s - Comparison between the analytical solution (—) and the simulation (- - -) with the MacCormack TVD scheme. 200 grid points are computed with  $\Delta t = 0.01$ .

Rewriting the (SV) equations in a pair of characteristic equations and taking into account the constant slope topography, we can obtain Riemann invariants. Then, using a separation of the variables method, we obtain an implicit solution to the non-linear run-

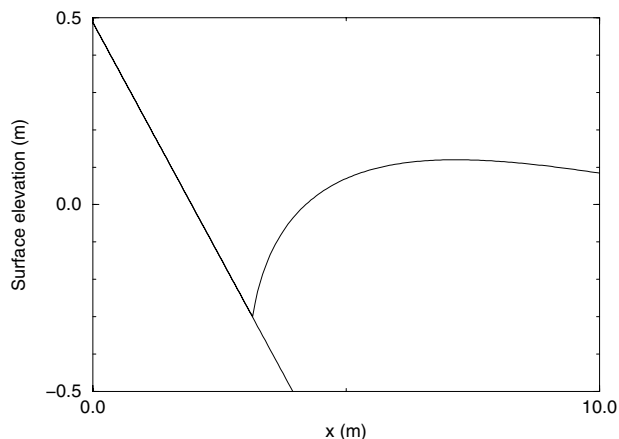


Fig. 8. Initial condition of the run-up problem -  $u = 0$  and  $h$  is chosen at the moment when the dry beach zone is the largest

up problem, which can be solved, for instance, with a Gauss-Seidel iterative algorithm.  $T$  is the wave period,  $A$  is the wave amplitude and  $\frac{\partial Z_f}{\partial x} = \tan\theta$  is the beach slope. Non-breaking waves solutions can be obtained from the SV equations when the breaking criterion

$$A < \frac{g(\tan\theta T)^2}{4\pi^2}$$

is respected; the maximum run-up is obtained when  $x = \frac{A}{\tan\theta}$ . The initial condition of the problem (fig. 8) corresponds to the maximum wave steepening of the analytical solution ( $u = 0$  m/s). The parameters are chosen as follow:  $A = 0.3$  m,  $\theta = \frac{\pi}{8}$  and  $T = 5$  s. The numerical computations were done with a minimum water depth of  $10^{-4}$  m on the beach. A grid of 200 points was used, with  $\Delta t = 0.005$  s. At the seaward boundary, we impose the analytical solution. A comparison between the numerical solution and the analytical one is shown on fig. 11. The non-linear wave climbing the beach of constant slope is calculated in close accordance with the Carrier and Greenspan analytical solution. The calculated surface evolutions (see fig. 9-upper graph) and the velocity profiles (see fig. 9-lower graph) are almost equal to the theoretical solution.

If we examine more precisely the solutions near the shoreline, we can notice that the maximum numerical solving error occurs near the maximum and minimum run-up. Indeed, in this zone, the shoreline accelerates quickly, with a velocity increasing from 0 to 1.5 m/s when  $0 \leq \frac{t}{T} \leq 0.125$ , which is very short with respect to the wave period. An almost periodic behaviour of the approximation error on the shoreline position is observed (see fig. 10). We can verify that the differences between the numerical and the theoretical solutions are increased near the maximum and minimum run-up shoreline zone. Between these two states, the errors become smaller and smaller. On the other hand, better accuracy is obtained when the velocities and the accelerations decrease. The approximation errors cause a slight delay due to the order 1 of our TVD scheme in the shoreline zone and to the thin water layer kept at the slope. However, the global numerical solution obtained remains very satisfying: no oscillations appear, whereas the velocity profiles are discontinuous, and the results are more accurate than those of Hibbert and Peregrine [10].

## 6 Bore propagation on a sloping beach

The climb of a bore on a beach is investigated to illustrate the ability of the MacCormack TVD scheme to simulate typical wave propagation on beaches. The simulation describes an incident bore of 0.5 m height during one running-up and back-washing process onto a beach having a 2% slope. The results on 250 grid points are presented on fig. 11. The domain length is 250 m. The bore is initiated by a dam-break, seaward to the beach.

Before the back-wash process, two major phases are encountered: on the one hand, during the collapse of the bore, the velocity quickly increased whereas the bore spreads onto the beach ( $t = 16$  s and  $t = 20$  s); on the other hand, during the run-up, the bore vanishes and the velocity decreases progressively ( $t = 28$  s,  $t = 36$  s and

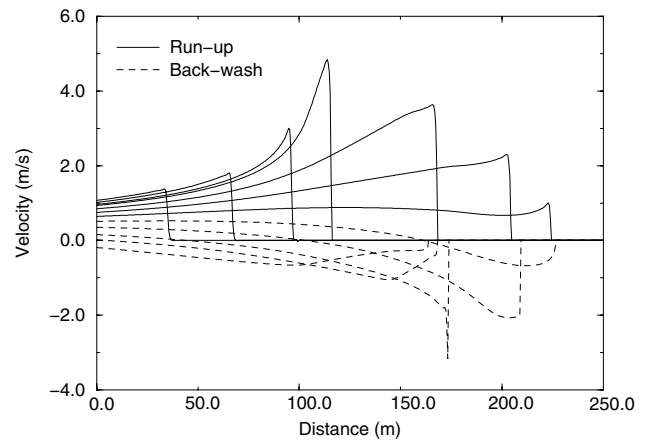
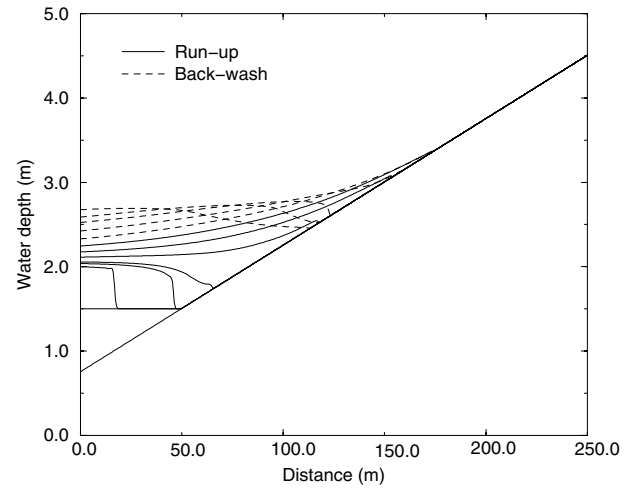
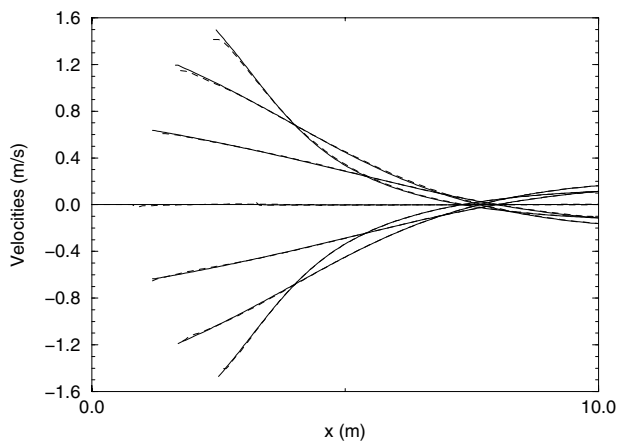
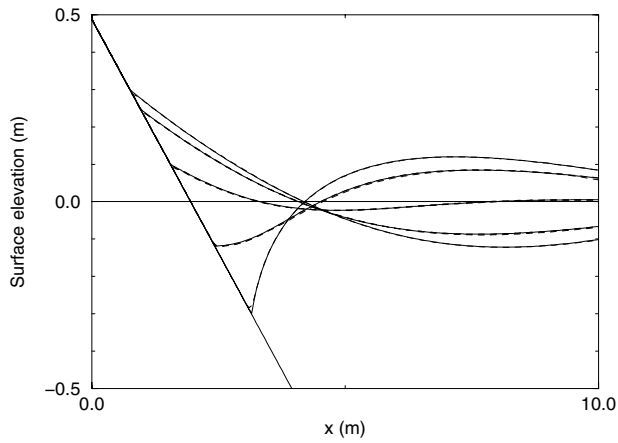


Fig. 9. Comparison of the MacCormack TVD scheme (---) with the analytical solution of Carrier and Greenspan [4] (—) - the results are shown every 125 iterations during 5 seconds - the figure describes the water surface evolutions (upper graph) and the velocity profiles (lower graph). 200 grid points are computed with  $\Delta t=0.005$ .

Fig. 11. Climb of a bore on a beach - the numerical results correspond to the times 0 s, 8 s, 16 s, 20 s, 28 s, 36 s, 40 s, 44 s, 48 s, 56 s, 60 s and 64 s - the figure describes the water surface evolutions (upper graph) and the velocity profiles (lower graph). 250 grid points are computed with  $\Delta t=0.02$ .

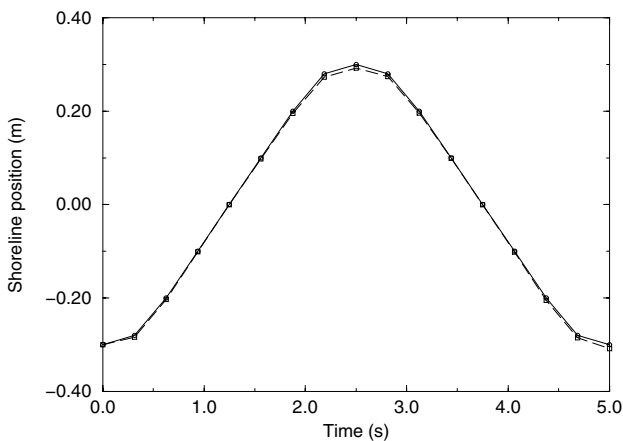


Fig. 10. Evolution of the analytical and the calculated shoreline position on one run-up period.

$t=40$  s) until the equilibrium between gravity and inertia is reached. Then, the flow is fully dominated by gravity and the back-wash is initiated with strong velocities, which are oriented seaward ( $t=44$  s and  $t=48$  s). The seaward water, which moves more slowly than the back-wash water creates a back-wash bore, animated by a strong velocity peak ( $t=56$  s). This bore quickly disappears as the water is evacuated to the sea.

The results presented in this section agree closely with those of Hibbert and Peregrine [10]. Nevertheless, our calculated transition from bore to run-up is less smooth and progressive than that of Hibbert and Peregrine's. Following the work of Yeh et al [22], we can maintain that the Hibbert and Peregrine scheme is too diffusive and provides low precision solutions of the problem near the shoreline.

## 7 Conclusion

The use of the Saint-Venant equations to simulate strongly non-linear coastal hydrodynamic free-surface flows, like bore propagation on a sloping beach with an important run-up and back-wash, needs specific mathematical calculation to correctly solve the problem. The high order non-oscillatory Mac Cormack TVD scheme presented in this article is a shock-capturing method appropriate to describe bore propagation and run-up on beaches, without introducing numerical dissipation near the wave fronts. Since these fronts are supposed to physically represent an area where energy is dissipated by turbulence motions, it would be necessary to add locally turbulent dissipation based on physical arguments (e.g. Svendsen and Madsen [18]). This method could be an alternative to those of Hibberd and Peregrine [10] and Kobayashi et al. [12], where the physical dissipation is replaced by an important numerical dissipation, which introduces a dependency of the results on the numerical resolution.

## Acknowledgment

This work was financially supported by the PNOC program (Programme National d'Océanographie Côtière) and by Conseil Régional d'Aquitaine.

## Notations

<b>q</b>	vector of conservative variables
<b>F</b>	flux vector
<b>S</b>	source term
<b>A</b>	Jacobian matrix
<b>L</b>	length of the calculation domain
<b>R</b>	right-eigenvector matrix
<b>U</b>	velocity in the x direction
<b>C</b>	wave celerity
<b>H</b>	total water depth
<b>Z<sub>f</sub></b>	bottom topography
<b>h<sub>1</sub></b>	water level left to the dam
<b>h<sub>2</sub></b>	water level right to the dam
<b>g</b>	gravity acceleration
<b>Fr</b>	Froude number

## References

[1] AMBROSI, D. (1995) "Approximation of shallow water equations by Roe's Riemann solver", Int. j. numer. methods fluids, 20, pp. 157-168

[2] BONNETON, P., CALTAGIRONE, J-P., Vincent, S. and Abadie, S. (1997) "Modélisation de l'hydrodynamique sédimentaire en zone côtière", proc. Bordomer97, 2, pp. 287-297.

[3] BONNETON, P., VINCENT, S., DUPUIS, H. and PEDREROS, R. (1999) "Modelling of wave transformation across the inner surf zone and swash oscillations on beaches", proc. 4<sup>th</sup> Int. Conf. Comput. Modelling of Seas and Coastal Regions, Wit Press, pp. 77-86.

[4] CARRIER, G.F. and GREENSPAN, H.P. (1957) "Water waves of finite amplitude on a sloping beach, J. Fluid Mech., 4, pp. 97-109

[5] CHINNAYYA, A. and LE ROUX, A. Y. (1999) "A new general Riemann solver for the Shallow water equations, with friction and topography", preprint of the Institut for Matematiske FAC, NTNU Trondheim , pp. 1-63

[6] GARCIA, R. and KAHAWITA, R.A. (1986) "Numerical solution of the St. Venant equations with the Mac Cormack finite-difference scheme", Int. J. Numer. Methods Fluids, 6, pp. 259-274

[7] GARCIA-NAVARRO, P., ALCRUDO, F. and SAVIRON, J.M. (1992) "1-D open channel flow simulation using TVD-McCormack scheme", J. Hydr. Eng., 118, pp. 1359-1372

[8] GLAISTER, P. (1993) "Flux difference splitting for open-channel flows", Int. j. numer. methods fluids, 16, pp. 629-654

[9] HARTEN, A. (1984) "A study of numerical methods for hyperbolic conservation laws with stiff source terms On a class of high-resolution total variation stable finite difference schemes", SIAM J. Numer. Anal., 21, pp. 1-23

[10] HIBBERT, S. and PEREGRINE, D.H. (1979) "Surf and run-up on a beach: a uniform bore", J. Fluid Mech., 95, pp. 323-345

[11] HIRSCH, C. (1990) "Numerical computation of internal and external flows", John Wiley and sons

[12] KOBAYASHI, N., DESILVA, G.S. and WATSON, K.D. (1989) "Wave transformation and swash oscillation on gentle and steep slopes", J. Geophys. Res., 94, pp. 951-966.

[13] LEVEQUE, R.J. and YEE, H.C. (1990) "A study of numerical methods for hyperbolic conservation laws with stiff source terms", J. Comput. Phys., 86, pp. 187-210

[14] LIU, P.L.-F., SYNOLAKIS, C.E. and YEH, H.H. (1991) "Report on the International Workshop on long-wave run-up", J. Fluid Mech., 229, pp. 675-688

[15] MEI, C.C. (1989) "The applied dynamics of ocean surface waves", Advanced Series on Ocean Engineering, 1, world scientific

[16] NUJIC, M. (1995) "Efficient implementation of non-oscillatory schemes for the computation of free surface flows", J. Hydr. Res., 33, pp. 101-111

[17] ROE, P.L., (1981) "Approximate Riemann solvers, parameter vectors and difference schemes", J. Comp. Phys., 43, pp. 357-372

[18] SVENDSEN, I.A. and MADSEN, P. (1981) "Energy dissipation in hydraulic jumps and breaking waves.", Progress Report No 55, Inst. of Hydrodynamic and Hydraulic Engineering, ISVA , Techn. Univ. Denmark, pp. 39-47.

[19] WANG, L.X. (1987) "Composite-model of 1-d and 2d flows", Advanced course and workshop on mathematical modeling of alluvial river, IRTCES-Beijing, China

[20] WHITAM, G.B. (1974) "Linear and non-linear waves", Wiley-Interscience Publication

[21] YEE, H.C. (1987) "Upwind and Symmetric Shock-Capturing Schemes", NASA Technical Memorandum, 89464

[22] YEH, H.H., GHAZALI, A. and MARTON, I. (1989) "Experi-

mental study of bore run-up", J. Fluid Mech., 206, pp. 563-578

[23] ZHAO, D.H., SHEN, H.W., TABIOS, G.Q., LAI, J. and TAN, W.Y. (1994) "Finite-volume two-dimensional unsteady-flow model for river basins", J. Hydr. Eng., 120, pp. 863-883

## 8 Appendix

Defining the Jacobian matrix of  $\mathbf{A}$  as

$$\mathbf{A} = \frac{\partial \mathbf{F}}{\partial \mathbf{q}} = \begin{pmatrix} 0 & 1 \\ -u^2 + c^2 & 2u \end{pmatrix}$$

where  $c = \sqrt{gh}$ , the system becomes:

$$\frac{\partial \mathbf{q}}{\partial t} + \mathbf{A} \frac{\partial \mathbf{q}}{\partial x} = \mathbf{S}$$

Studying the characteristic polynomial of  $\mathbf{A}$ , we get

$\det(\mathbf{A} - a\mathbf{I}) = -(a-u)(-a^2 + 2au - u^2 + gh)$ , which leads to the corresponding eigenvalues  $a = \left(\frac{u-c}{u+c}\right)$  and right eigenvectors  $\begin{pmatrix} 1 \\ u-c \end{pmatrix}$  and  $\begin{pmatrix} 1 \\ u+c \end{pmatrix}$ .

The right eigenvector matrix  $\mathbf{R}$  of the Jacobian matrix  $\mathbf{A}$  and its

inverse are written as  $\mathbf{R} = \begin{pmatrix} 1 & 1 \\ u-c & u+c \end{pmatrix}$  and  $\mathbf{R}^{-1} = \begin{pmatrix} \frac{u+c}{2c} & \frac{-1}{2c} \\ \frac{-u+c}{2c} & \frac{1}{2c} \end{pmatrix}$ .

To determine the Riemann problem Roe [17] suggested that the following conditions should be imposed on  $\mathbf{A}$ :

(i) the system is strictly hyperbolic; as a consequence, the Jacobian matrix  $\mathbf{A}$  is diagonalizable with real eigenvalues.

(ii)  $\mathbf{A}_{i+1/2}(\mathbf{q}_i, \mathbf{q}_{i+1}) \rightarrow \mathbf{A}(\mathbf{q}) = \frac{\partial \mathbf{F}}{\partial \mathbf{q}}$

(iii)  $\mathbf{A}(i+1/2)(\mathbf{q}_{i+1} - \mathbf{q}_i) = \mathbf{F}(\mathbf{q}_{i+1}) - \mathbf{F}(\mathbf{q}_i)$

It is well known that the shallow water equations leads to a strictly hyperbolic system ((i) is correct). To satisfy (iii), we have to express  $u_{i+1/2}$  and  $h_{i+1/2}$ . However,  $\mathbf{A}$  is fully non-linear and we cannot directly estimate the unknown variables at the interface. Roe's idea is to break up  $\mathbf{A}$  in the multiplication of two linear matrix. The vectors  $\mathbf{q}$  and  $\mathbf{F}$  can be expressed as quadratic functions of the variable  $\mathbf{W}$  defined by

$$\mathbf{W} = \sqrt{h} \begin{pmatrix} 1 \\ u \end{pmatrix}; \quad \mathbf{q} = \begin{pmatrix} w_1^2 \\ w_1 w_2 \end{pmatrix} \text{ and}$$

$$\mathbf{F} = \begin{pmatrix} w_1 w_2 \\ w_2^2 + \frac{g}{2} w_1^4 \end{pmatrix}$$

We can find a projection matrix  $\mathbf{B}$  between  $\mathbf{q}$  and  $\mathbf{W}$  verifying

$$\mathbf{q}_{i+1} - \mathbf{q}_i = \mathbf{B}(\mathbf{W}_{i+1} - \mathbf{W}_i)$$

where

$$\mathbf{B} = \begin{pmatrix} 2\bar{w}_1 & 0 \\ \bar{w}_2 & \bar{w}_1 \end{pmatrix}.$$

The notation  $\bar{k} = \frac{k_{i+1} + k_i}{2}$  represents an arithmetic verage.

An analogous calculation gives the crossing matrix  $\mathbf{C}$  between  $\mathbf{F}$  and  $\mathbf{W}$

$$\mathbf{F}_{i+1} - \mathbf{F}_i = \mathbf{C}(\mathbf{W}_{i+1} - \mathbf{W}_i)$$

where  $\mathbf{C} = \begin{pmatrix} \bar{w}_2 & \bar{w}_1 \\ 2g(\bar{w}_1^2 + \bar{w}_1^2) & \bar{w}_1 \bar{w}_2 \end{pmatrix}$  and  $\tilde{k} = \frac{k_{i+1} - k_i}{2}$ .

We can observe that  $\mathbf{q}$  and  $\mathbf{F}$  are homogeneous functions of degree two in  $\mathbf{W}$  while  $\mathbf{B}$  and  $\mathbf{C}$  are homogeneous of degree one in  $\mathbf{W}$ . As  $\mathbf{B}^{-1}(\mathbf{q}_{i+1} - \mathbf{q}_i) = (\mathbf{W}_{i+1} - \mathbf{W}_i)$ , we can express  $\mathbf{q}$  according to  $\mathbf{F}$ :

$$\mathbf{F}_{i+1} - \mathbf{F}_i = \mathbf{C}\mathbf{B}^{-1}(\mathbf{q}_{i+1} - \mathbf{q}_i)$$

Using (iii), we get

$$\mathbf{F}(\mathbf{q}_{i+1}) - \mathbf{F}(\mathbf{q}_i) = \mathbf{A}_{i+1/2}(\mathbf{q}_{i+1} - \mathbf{q}_i)$$

Identifying the previous formulas, we find the linearised expression which allows us to calculate  $\mathbf{A}$  by a linear matrix multiplication:  $\mathbf{A}_{i+1/2} = \mathbf{C}\mathbf{B}^{-1}$ .

Knowing

$$\mathbf{B}^{-1} = \begin{pmatrix} \frac{1}{2\bar{w}_1} & 0 \\ \frac{\bar{w}_2}{\bar{w}_1^2} & \frac{2}{\bar{w}_1} \end{pmatrix}$$

we find the unknown variables estimated in  $i+1/2$  as Roe's averages:

$$h_{i+1/2} = \frac{h_{i+1} + h_i}{2}$$

$$u_{i+1/2} = \frac{\sqrt{h_{i+1}}u_{i+1} + \sqrt{h_i}u_i}{\sqrt{h_{i+1}} + \sqrt{h_i}}$$